

## Supplementary Material

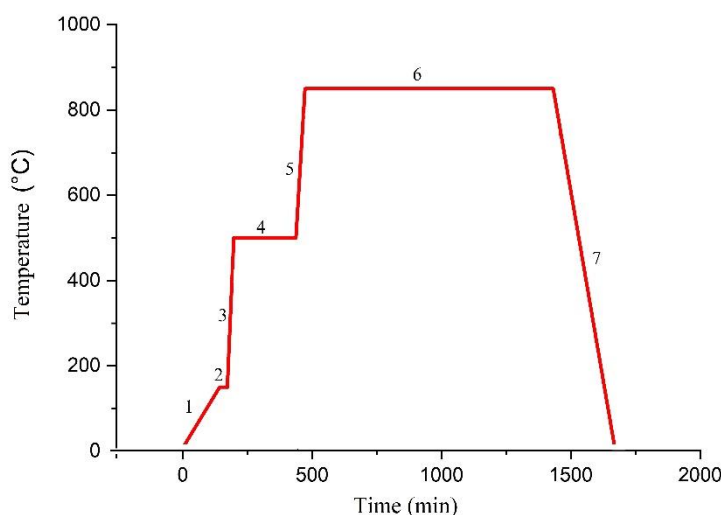


Figure S1. The diagram of the heat treatment stages.

During the first stage, slow heating occurs at a rate of 1 °C/min to a site of 150 °C. During this heating, adsorbed water and bound water from acetates were released from the precursor. When choosing the heating rate, two fundamental factors were taken into account: the first – the heating should not be too fast so that the process of evaporation of residual moisture from the gel has time to pass before the next reaction begins. Also, slow heating makes it possible to reduce the intensity of the release of gaseous products during the initial decomposition reactions of the precursor, since active gas release can remove solid reagents from the reaction medium, which will affect the final product of the reaction.

In the second stage, a temperature value of 150 °C is maintained for 30 minutes to completely evaporate the residual water from the precursor.

During the third stage, heating occurs from 150 °C to 500°C with a heating rate of 10°C/min. During this stage, the process of decomposition of malic acid and acetates of nickel, manganese and lithium begins, most of the carbon is removed from the material in the form of CO and CO<sub>2</sub>.

In the fourth stage, a constant temperature value of 500°C is maintained for 4 hours, at which the pyrolysis of malic acid occurs and the formation of crystalline NCM begins.

During the 5th stage, heating occurs from 500 °C to 850 °C with a heating rate of 10°C/min.

At the sixth stage, at 850 °C, the mixture is calcined, and the formation of a triple lithium oxide of transition metals ends. The choice of such a temperature for calcining the mixture is justified by the fact that at lower processing temperatures, the synthesized material demonstrates an inhomogeneous particle distribution and fuzzy grain boundaries, the layered structure is not fully formed. At temperatures above

850°C, the particle size of the synthesized powder becomes larger, large "secondary" particles are formed, which in turn worsens the diffusion of lithium ions, and accordingly increases the polarization of the electrode and worsens the electrochemical properties.

At stage 7, the synthesized material is passively cooled.

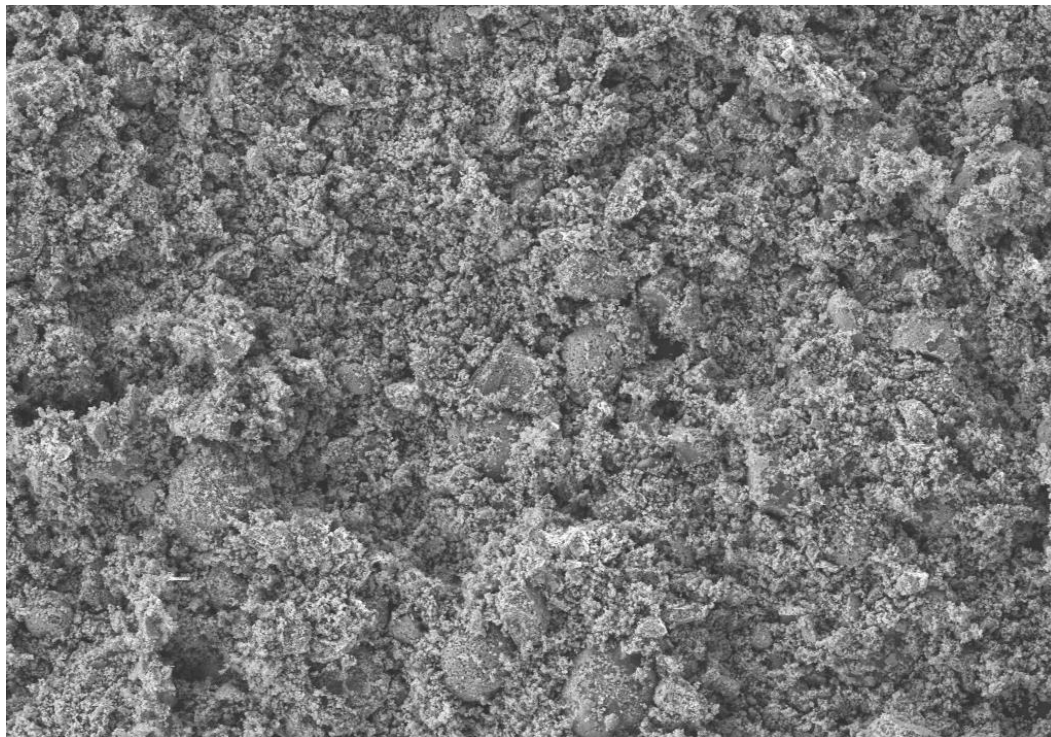


Figure S2. The SEM image of initial LCO material.

To determine the amount of extracted cobalt depending on leaching time, the elemental composition was analyzed by the EDX method. The results are shown in Table S1.

Table S1. Averaged results of elemental analysis of 5 samples of synthesized material in at.%

Specimen	C	O	Al	P	Fe	Co	Ni
1	7.28	44.19	0.41	0.34	-	<b>14.94</b>	<b>32.84</b>
2	5.75	43.51	0.52	0.47	0.67	<b>21.06</b>	<b>28.02</b>
3	7.48	44.05	0.68	0.58	0.63	<b>20.31</b>	<b>26.27</b>
4	15.70	44.10	0.72	0.47	0.58	<b>16.93</b>	<b>21.50</b>
5	7.29	46.72	0.89	0.58	0.66	<b>19.06</b>	<b>24.81</b>

Based on the obtained values, a dependence graph of the mass of extracted cobalt in the sample on the leaching time was constructed. The cobalt masses were calculated based on the Co/Ni ratio in the sample. The graph is shown in Figure S3.

As it can be seen, after 60 minutes, the cobalt mass reaches a plateau, which suggests that further leaching is impractical. Thus, during the subsequent cobalt extraction experiments, the leaching time was 60 minutes.

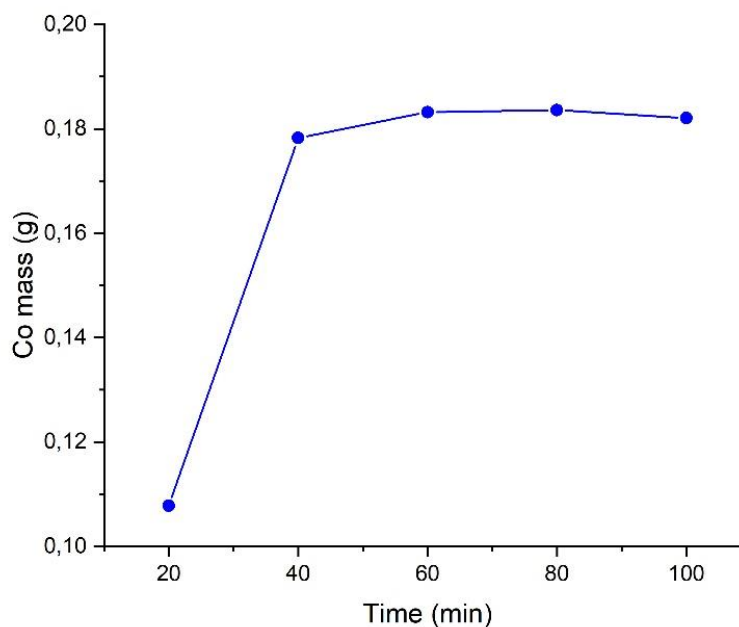


Figure S3. The dependence of the extracted mass of cobalt on the leaching time.

The values of the crystal lattice parameters for commercial and synthesized material are presented in Table S2. The lattice parameters differ slightly, which indicates a low amount of impurities in the synthesized material and good crystallinity. The value of microstresses is quite small, respectively, there are no microstresses in the synthesized NCM111, which contributes to good lithium diffusion during intercalation and deintercalation processes. High values of the  $c/a$  ratio, as well as the I003/I104 ratio, indicate a well-formed hexagonal layered structure. Thus, it can be concluded that sol-gel synthesis with subsequent heat treatment makes it possible to obtain a cathode material of the NCM type with characteristics comparable to commercial materials.

Table S2. Structural parameters of crystal lattices for commercial and synthesized material.

NCM111	$a$ , (Å)	$c$ , (Å)	$c/a$	$e_0$	CSR, nm
Commercial	2.864	14.245	4.974	0.0007	>150
Synthesized	2.861	14.232	4.974	0.0006	58

In Table S3 the structure parameters of both materials lattices are presented. The values of microstresses for these materials are higher than for commercial NCM111, but not critical. At the same time, the SCR for all materials is more than 150-200 nm.

Table S3. Structural parameters of crystal lattices for NCM622 and NCM811.

	$a$ , (Å)	$c$ , (Å)	$c/a$	$\epsilon_0$	SCR, nm
NCM622	2.874	14.237	4.953	0.001	>150
NCM811	2.875	14.214	4.944	0.001	>200

Table S4. Sample modeling parameters.

	25.1.3	25.6.1		26.8.3
R1	8.2176	6.4966	R1	5.1409
CPE1_T	2.02E-05	1.89E-05	CPE1_T	7.27E-05
CPE1_P	0.84326	0.84044	CPE1_P	0.709
R2	74.368	223.91	R2	5.5951
W1_R	56.59	179.86	CPE2_T	0.00349
W1_T	1.37E+07	1774.5	CPE2_P	1.228
W1_P	0.14573	0.30275	R3	9.2543
			CPE3_T	0.00687
			CPE3_P	1.133
			R4	23.798
			W1_R	144.91
			W1_T	77.66
			W1_P	0.35745